J. Biochem. **134**, 731–738 (2003)
DOI: 10.1093/jb/mvg201

Interaction between Pyridoxal Kinase and Pyridoxal-5-phosphate–Dependent Enzymes

Pik-Yuen Cheung[1], Chi-Chun Fong[2], Kang-To Ng[1], Wan-Chuen Lam[1], Yun-Chung Leung[1], Chun-Wai Tsang[1], Mengsu Yang[*,2] and Man-Sau Wong[†,1]

[1]The Central Laboratory of the Institute of Molecular Technology for Drug Discovery and Synthesis, Department of Applied Biology and Chemical Technology, The Hong Kong Polytechnic University, Hung Hom, Kowloon, Hong Kong SAR, P.R.C.; and [2]Department of Biology and Chemistry, City University of Hong Kong, 83 Tat Chee Avenu, Kowloon, Hong Kong SAR, P.R.C.

Received June 18, 2003; accepted September 9, 2003

The interactions of two pyridoxal-5-phosphate (PLP)–dependent enzymes, alanine aminotransferase (ALT) and glutamate decarboxylase (GAD), with pyridoxal kinase (PK) were studied by fluorescence polarization as well as surface plasmon resonance techniques. The results demonstrated that PK can specifically bind to ALT and GAD. Moreover, binding profiles of both enzymes to immobilized PK were altered by excess amount of PLP. The equilibrium affinity constants for ALT in the absence and presence of PLP are 20.4×10^4 $M^{-1}$and 6.7×10^4 M^{-1}, and for GAD are 37×10^4 $M^{-1}$and 20.8×10^4 M^{-1}, respectively. It appears that specific interactions occur between PK and PLP-dependent enzymes, and the binding affinities of PK for PLP-dependent enzymes decrease in the presence of PLP. The results support our hypothesis that PLP transfer from PK to PLP-dependent enzymes requires a specific interaction between PK and the enzyme.

Key words: alanine aminotransferase, glutamate decarboxylase, pyridoxal kinase, pyridoxal-5-phosphate–dependent protein, surface plasmon resonance.

Abbreviations: ALT, alanine aminotransferase; GABA, γ-aminobutyric acid; AST, aspartate aminotransferase; EDC, *N*-ethyl-*N*′-(3-diethylaminopropyl)carbodiimide; FMI, fluorescein-5-maleimide; GAD, glutamate decarboxylase; NHS, *N*-hydroxysuccinimide; PK, pyridoxal kinase; PL, pyridoxal; PLP, pyridoxal-5-phosphate; SPR, surface plasmon resonance.

Pyridoxal-5-phosphate (PLP) is the active form of vitamin B_6 [pyridoxal (PL), pyridoxine and pyridoxamine]. PLP is frequently described as nature's most versatile coenzyme and is required for numerous enzymes (PLP-dependent enzymes) that catalyze a large array of reactions in the synthesis, catabolism, and interconversion of amino acids (*1*, *2*). A recent study by Denesyuk *et al.* (*3*) showed the importance of the phosphate group binding cup for the catalytic activities of PLP-dependent enzymes. The cellular content of PLP is determined by the function of pyridoxal kinase (PK), pyridoxine-5-phosphate oxidase and phosphatases. The scheme for the interconversion of B_6 vitamers with their 5′-phospho forms including the coenzyme PLP has been shown by McCormick *et al.* (*4*) to illustrate the central role of both the kinase and oxidase in vitamin B_6 metabolism.

PK is an important enzyme that has been detected in many different organisms and in virtually all mammalian tissues including the brain (*5*). It is a dimer having identical subunits of 40 kDa that consists of two domains responsible for ATP and PL binding (*6*). The three dimensional structures of sheep brain PK and its complex with the nucleotide ATP were elucidated recently (*7*). PK phosphorylates PL to form PLP in the presence of ATP and a divalent cation (Zn^{2+}) in liver, PLP is then released to the bloodstream in association with albumin via Schiff-base linkage (*8*). K^+ was reported to have a stimulatory effect on PK in bovine brain (*5*), human erythrocytes (*9*), and porcine brain (*10*). Circulating PLP is dephosphorylated by membrane-associated phosphatases before gaining entry to target cells (*11*, *12*) and being converted back to the active cofactor by intracellular PK after passing through the cell membrane.

A low PLP level is maintained in the cell by hydrolysis, and yet a vast number of enzymes depend on PLP for their enzymatic activities. Therefore, how PLP is transported to the PLP-dependent enzymes without depletion, and how a single enzyme can react with such a large number of diverse enzymes, are matters of interest. A previous study had shown that PK interacts with aspartate aminotransferase (AST) (*13*), indicating compartmentation of PLP might occur to prevent its degradation.

The delivery of PLP from PK to PLP-dependent apoenzyme is a crucial step for ensuring the proper functioning of a large number of vitamin B_6-dependent enzymes. We hypothesize that specific interactions between PK and PLP-dependent enzyme is essential for PLP transfer. In this study, interactions of two PLP-dependent enzymes, alanine aminotransferase (ALT) and glutamate decarboxylase (GAD), with PK were first studied by fluorescence polarization technique, followed by surface plasmon resonance (SPR) biosensor technology. GAD is a

[*]To whom correspondence should be addressed. Fax: +852-2788-7406, E-mail: bhmyang@cityu.edu.hk
[†]To whom correspondence should be addressed. Tel: +852-27666695, Fax: +852-23649932, E-mail: bcmswong@polyu.edu.hk

hexamer having a molecular mass of 310 kDa (*14*) and subunits of 50 kDa, each of which binds to one molecule of PLP (*15*). It catalyzes α-decarboxylation of L-glutamic acid to form γ-aminobutyric acid (GABA), a major neurotransmitter in the vertebrate central nervous system (*16*). ALT is a homodimer having a molecular mass of 100 kDa and subunits of 50 kDa, each of which binds to one molecule of PLP. It catalyzes transamination between alanine and 2-oxoglutarate to form pyruvate and glutamate, which participates in nitrogen metabolism and liver gluconeogenesis (*17*). Fluorescence polarization study used fluorescent-labeled PK to monitor its interaction with ALT or GAD in solution in the equilibrium state, whereas the SPR biosensor could monitor biomolecular interaction in real time and determine binding kinetics and affinities without using radioactive or fluorescent-labeled ligands (*18*, *19*). The effects of PLP on binding interaction of PK with ALT and GAD were also investigated with the SPR biosensor. The SPR results provide kinetic parameters related to the binding mechanism of the enzymes. This information is invaluable for understanding the regulatory pathway of PLP transfer. The binding of these two PLP-dependent enzymes with PK could also serve as models for studying the interaction of PK with other PLP-dependent enzymes.

MATERIALS AND METHODS

Materials—The BIAcore*X*™ instrument, sensor chip (CM5, research grade), HBS buffer (10 mM HEPES, 150 mM NaCl, 3.4 mM EDTA, 0.05% P20, pH 7.4) and the amine coupling kit containing *N*-hydroxysuccinimide (NHS), *N*-ethyl-*N*′-(3-diethylaminopropyl)carbodiimide (EDC) and ethanolamine hydrochloride were from Pharmacia Biosensor (Uppsala, Sweden). Potassium hydrogen phosphate, potassium dihydrogen phosphate, potassium chloride, sodium dodecyl sulfate (SDS) and hydrochloric acid were from Honeywell Specialty Chemicals (Seelze, Germany). Porcine heart ALT, *E. coli* GAD and PLP were from Sigma (St. Louis, MO, USA). Fluorescein-5-maleimide was from Molecular Probes (Eugene, USA). Acetonitrile and formic acid were from Merck, (Merck, Germany).

Purification of Recombinant Porcine PK and GAD—Porcine PK was expressed in *E. coli*, and purified to more than 95% purity according to the method developed in our laboratory (*10*) through ammonium sulfate precipitation (50 % saturation) and Q-Sepharose ion-exchange.

The purchased GAD was purified by passage through a Superdex-200 prep grade HiLoad 16/60 column on an ÄKTA explorer purification system (Amersham Biosciences, Uppsala, Sweden). Purification was carried out at 4°C. Purchased GAD was dissolved in the elution buffer (PB, 50 mM potassium phosphate buffer containing 150 mM potassium chloride, pH 6.8) and loaded onto the column. Elution was carried out at a flow rate of 1 ml/min for 1.3 column volumes, and fractions of 1 ml were collected. Protein concentration of eluted sample was monitored at 280 nm throughout the elution process using the ÄKTA explorer. More than 70% purity was achieved after this step as judged by the SDS-PAGE.

Mass Determination of GAD and ALT—Electrospray ionization time of flight mass spectrometry (Q-TOF II, Micromass, Altrincham, U.K.) was used to determine the mass of GAD and ALT to determine the ratio of the apo and holo forms of the enzymes used in this study. Protein sample (GAD or ALT) at a concentration of 10^{-4} M was dissolved in 50% acetonitrile mixture acidified with 1% formic acid and sprayed through a capillary elevated at a potential of 2.2 to 3 kV. Horse heart myoglobin was used as the standard for calibration and mass spectrum was scanned between the range of 600–1,600 m/z.

Labeling of PK—PK (20 μM) was allowed to react with 5 mM fluorescein-5-maleimide (FMI) in 50 mM potassium phosphate (pH 6.8). The mole ratio of enzyme : fluorescein was approximately 1:10. The reaction was allowed to proceed for 4 h at 4°C with stirring. Excess of free reagent was removed by dialysis against the same buffer at 4°C. The degree of labeling of PK was determined spectrophotometrically using an extinction coefficient of 83,000 M^{-1} cm^{-1} at 495 nm. The incorporation of 1.1 mol of dye/monomer does not affect the catalytic function of PK.

Fluorescence Polarization Study on the Interaction between PK and PLP-Dependent Enzymes—Labeled PK (1 μM) interacted with PLP-dependent enzymes ALT and GAD at various concentrations (0–20 μM) in PB. The mixture was allowed to stand for 5 min at 25°C after the addition of ALT or GAD in order to reach equilibrium. Fluorescence polarization intensity was measured by means of fluorescence spectroscopy using an excitation wavelength of 499 nm and an emission wavelength of 520 nm with a bandwidth of 5 nm. The fluorescence polarization intensity of labeled PK was used as the blank. Lysozyme interaction with labeled PK was included as a negative control.

The fraction (α) of FMI-PK bound to ALT or GAD is a function of P_0 (fluorescence polarization intensity of FMI-PK alone), P (fluorescence polarization intensity of FMI-PK-ALT/GAD) and Pm (maximum fluorescence polarization intensity). The following equations were used to analyze the interaction where the stoichiometry of the complex was assumed to be 1:1.

$$\alpha = (P - P_0)/(P_m - P_0) \quad (1)$$

The apparent equilibrium constant (dissociation constant) of the complex was determined by plotting 1/α against 1/[A] using Eq. 2.

$$1/\alpha = 1 + K/[A] \quad (2)$$

Where [A] is the concentration of the PLP-dependent enzyme and K is the apparent equilibrium constant. The values of dissociation constants for the binding interaction were obtained from duplicate experiments for each concentration of ALT/GAD.

Immobilization of PK on CM5 Sensor Chip—The basic principle of the SPR biosensor (BIAcore X) and some of its applications have been described in detail in the BIAtechnology Handbook (*20*) and elsewhere (*18*, *19*, *21*, *22*). CM5 sensor chips are pre-coated with carboxymethyl dextran, which can concentrate the ligand (PK) close to the surface of the chip for coupling. The effect of electrostatic interaction was studied by injecting the ligand in

coupling buffers at different pHs. The most suitable pH for coupling was determined to be pH 4.0.

Immobilization of PK was carried out by the standard amine coupling method as previously described (*10*, *23–25*). The immobilization procedures were carried out at 25°C at a constant flow rate of 5 μl/min. The carboxymethyl dextran surface in channel one was first activated by injecting 35 μl of 0.1 M EDC/0.1 M NHS premixed in 1:1 ratio prior to coupling. Then 35 μl of PK (10 μg/ml in 10 mM acetate coupling buffer, pH 4.0) was then injected over the activated surface for coupling, followed by the injection of 35 μl of 1 M ethanolamine to deactivate the remaining active carboxyl groups on the sensor chip surface. HCl (12 μl, 100 mM) was used to remove the remaining non-covalently bound PK. Similar activation and deactivation procedures were carried out for the control channel, except for the coupling procedure, where pH 4.0 coupling buffer was used in place of PK in order to block the remaining binding sites on the sensor chip surface and prevent non-specific binding. The control channel is used to correct non-specific binding and bulk refractive index change interference. The sensor chip was equilibrated at 5 μl/min with PB for 24 h before carrying out binding assays.

SPR Binding Interaction for PK and PLP-Dependent Enzymes—All binding experiments were carried out at 25°C with a constant flow rate of 8 μl/min using PB. ALT or GAD in PB ranging from 5 μM to 20 μM was injected over the sensor surface immobilized with PK for 3 min (association phase), followed by a 5-min wash with PB (dissociation phase). The sensor surface was then regenerated with either 100 mM HCl or 0.01 to 0.5% SDS. The interaction of PLP-dependent enzymes with PK was also studied in the presence of excess PLP (2 mM).

Kinetic Models and Data Analysis—The sensorgrams were analyzed with BIAevaluation™ Software version 3.0 (*26*). Several binding models were used to fit the PK-ALT or PK-GAD interaction data, including a simple one-to-one binding model (Langmuir), a heterogeneous analyte model (competing reactions) and a two state (conformational change) binding model with or without mass transport limit (*27*). The degree of randomness of the residual plot and the reduced χ^2 value were used to assess the appropriateness of a model to the sensor data. The simplest and the most appropriate model for each binding interaction was used to derive the kinetic parameters. It was found that the simple one-to-one binding model (Langmuir) provides sufficient fitting for the PK-ALT and PK-GAD interactions. This agrees with the fluorescence polarization study. The reaction equation for the model is described below, and its rate equation is used to fit the sensorgram data to derive binding kinetic constants.

Reaction equation:

$$A + B \underset{k_d}{\overset{k_a}{\rightleftharpoons}} AB \tag{3}$$

Rate equation:

$$\frac{d[AB]}{dt} = k_a[A][B] - k_d[AB] \tag{4}$$

Where A represents analyte in solution, B represents the ligand immobilized on sensor surface, AB is the complex formed by A and B, and k_a and k_d are their respective association and dissociation rate constants. The equilibrium affinity constant (K_A) and equilibrium dissociation constant (K_D) are calculated based on the ratio of k_a/k_d and k_d/k_a respectively.

Both the association and dissociation phases were fitted simultaneously. Data were fitted globally (fitting all concentrations simultaneously) and locally (fitting each concentration separately) to find the optimal fit for each binding interaction. Simultaneous local fit is optimal for the binding interaction. The mean values of the association and dissociation rate constants and equilibrium affinity constant of the binding interaction were obtained from duplicate experiments for each concentration of ALT/GAD with or without the presence of PLP.

Heterogeneous analyte and two-state binding models were also used to analyze the binding interaction. However, the use of these models did not improve the fitting for the binding interaction. The residual plots for the heterogeneous analyte model are included in the diagram for comparison. In simultaneous analysis, both association and dissociation were analyzed simultaneously, and association rate calculation depends on the dissociation rate. As the dissociation rate is very low, to eliminate the possibility of inaccurate calculation of association rate, BIAevaluation™ Software version 2.2 (*28*) was used to separately fit the association phase and compare the results with those obtained in version 3.0 model. The association model used was A + B = AB type 3. This model calculates $k_s = k_a C_n + k_d$ and initial binding rate r_0 by fitting data to the following equation:

$$R = (r_0/k_s)[1 - e^{-ks(t-t0)}] \tag{5}$$

Where n is the steric interference factor (default 1). By plotting k_s, the observed rate constant, against C, the sample concentration, k_a and k_d could be obtained.

RESULTS AND DISCUSSION

The cellular PLP level has been found to be very low, which is probably due to the high catalytic activity of both free and membrane bound phosphatases (*13*). This is consistent with the fact that the k_{cat} values of this large family of enzymes are at least 30-fold higher than that pertaining to pyridoxal kinase. It has been postulated that the hydrolysis of phosphorylated vitamin B_6 ensures that a low concentration of around 1 μM PLP is present in eukaryotic cells (*29*). Nevertheless, despite the existence of the active phosphatase, a considerable amount of PLP generated by the kinase is still available for binding to vitamin B_6-dependent enzymes. The underlying mechanism for the transfer of PLP to specific vitamin B_6-dependent apoenzymes in the presence of phosphatase is of interest.

Previous study by fluorescence spectroscopy showed that AST interacts with PK (*13*), and it is suggested that PLP transfer is achieved by compartmentalization. However, whether this interaction is specific to AST or general to all PLP-dependent enzymes is unknown. In the present study, fluorescence polarization study and SPR-based protein-protein interaction assay were developed for evaluation of the binding interaction between PK and

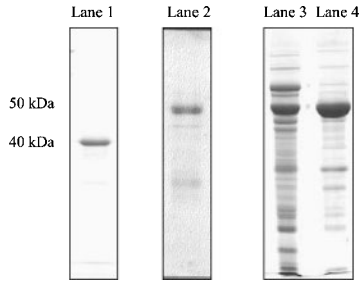

Fig. 1. **Purity of PK and PLP-dependent enzymes.** Protein samples of 5 μg were analyzed by 12% reducing SDS-PAGE and stained with Coomassie Blue. Lane 1 is PK, lane 2 is ALT, lane 3 is GAD before purification and lane 4 is the one-step purified GAD.

two PLP-dependent enzymes to determine whether the interaction is general or specific.

Purification of PK and GAD—Changes in fluorescence polarization intensity upon interaction of FMI-PK with ALT or GAD reflect changes in molecular volume and provide direct measurements of equilibrium binding. The SPR biosensor measures the mass changes as the analyte passes through the sensor chip surface. Both fluorescence polarization and SPR binding interactions would be affected by purity of the samples, because non-specific interaction increases with increasing impurity. To minimize non-specific interaction, samples of highest available purity should be used. The purity of the interacting proteins (PK, ALT, and GAD) is shown in Figure 1. PK was purified to homogeneity according to the method described. Both ALT and GAD were obtained commercially. The ALT was of acceptable purity (80%) for the analysis, and the GAD was too crude for the assay, and its purity was improved to 80% by a one-step purification using Superdex-200 prep grade column as indicated in lane 3 and lane 4 in Fig. 1.

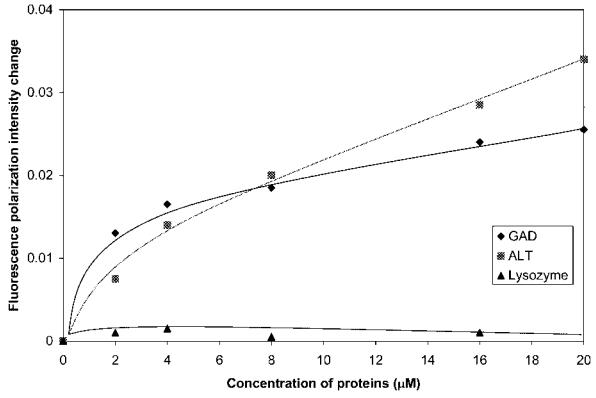

Fig. 2. **Interaction of FMI-PK with PLP-dependent enzymes.** Interactions of FMI-PK with various concentrations of PLP-dependent enzymes (0–20 μM) were monitored through fluorescence polarization intensity changes. The fluorescence polarization intensity was measured at an excitation wavelength of 499 nm and an emission wavelength of 520 nm with a bandwidth of 5 nm in PB containing a fixed concentration of FMI-PK (1 μM) at 25 °C. Fluorescence polarization intensity of FMI-PK was set as the blank, and the lysozyme interaction with FMI-PK was included as a negative control. Each point indicates the mean of duplicate measurement.

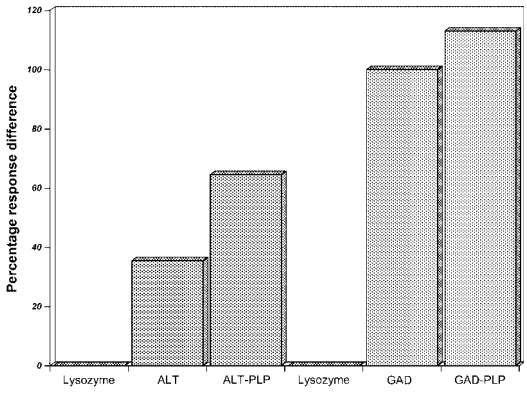

Fig. 3. **Chart showing the percentage response change for binding interactions of ALT and GAD with the immobilized PK.** Solutions of 5 μM ALT and GAD were injected onto biosensor chip surface immobilized with PK in the presence and absence of excess PLP (2 mM). The interaction was carried out at a flow rate of 8 μl/min and with an association phase of 3 min and dissociation phase of 5 min. Bar chart shows percentage response change for the binding interaction of ALT, and GAD with PK in the absence and presence of PLP after 3 min of binding. GAD interaction with PK was set as the reference with a percentage response difference of 100%. Lysozyme was included as the negative control.

Fluorescence Polarization Study—The purified enzymes were used in the fluorescence polarization study to determine if PK interacts with ALT or GAD. The fluorescence polarization intensity of FMI-PK increases with the increase in concentration of the PLP-dependent enzymes (Fig. 2). Both of these enzymes interact with PK, indicating that there is a general interaction between PK and PLP-dependent enzymes. The difference in molecular weight between GAD and ALT may be one of the reasons for the difference in fluorescence polarization intensity change. Lysozyme, a non-PLP-dependent protein that does not interact with PK was included as a negative control in the binding assay. By plotting $1/\alpha$ against 1/[A], the apparent equilibrium constants (dissociation constant) obtained for PK-ALT and PK–GAD are 5.6×10^{-6} M and 2.3×10^{-6} M, respectively.

SPR Biosensor Study—Fluorescence polarization study showed that there is a general interaction between PK and PLP-dependent enzymes. However, this method only studied binding interactions between enzymes at equilibrium. To monitor real-time binding interaction between purified PK and PLP-dependent enzymes, SPR biosensor study was performed. PK was immobilized onto the CM5 sensor chip using acetate coupling buffer at pH 4.0. Approximately 3.5 ng/mm^2 PK was immobilized based on the estimation that 1,000 RU corresponds to 1 ng/mm^2 of surface mass (*30*). A control surface was also prepared to correct for non-specific binding and bulk refractive index. Signals for specific binding interactions between immobilized PK and PLP-dependent enzymes (ALT and GAD) were generated by subtracting the non-specific signals from the control surface. This is the first time that quantitative kinetic profiles were obtained for the interactions between PK and PLP-dependent enzymes.

The binding interactions between immobilized PK and ALT or GAD were monitored in real time. Solutions of 5 μM ALT or GAD in the presence or absence of PLP were

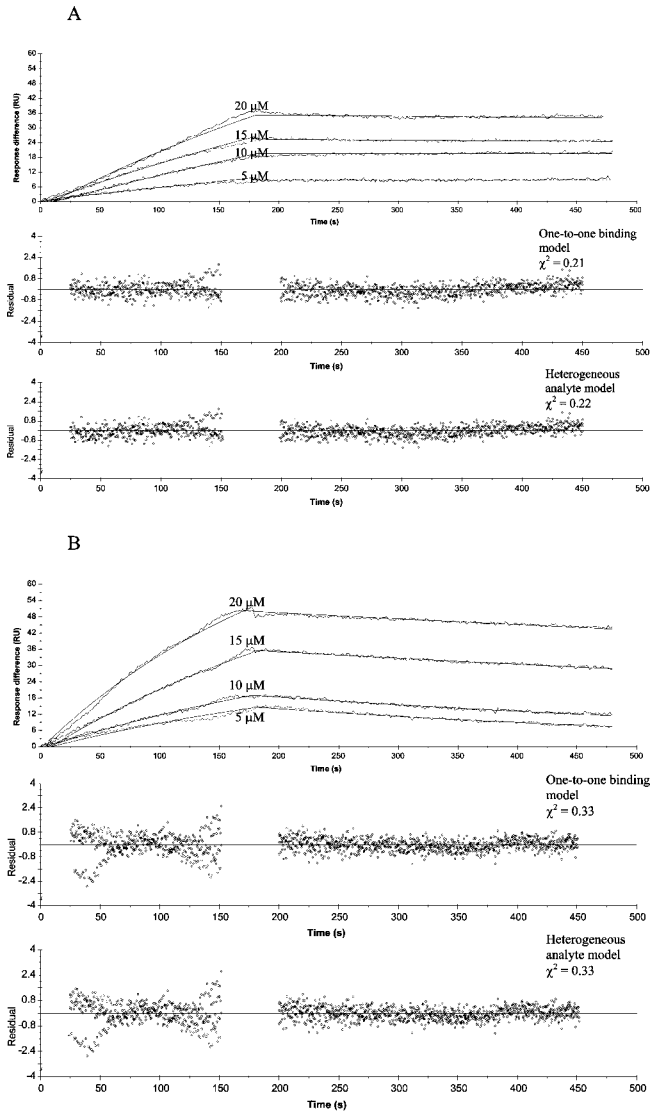

Fig. 4. **Sensorgrams showing the binding interactions of ALT with the immobilized PK.** Various concentrations of ALT (5–20 μM) were allowed to interact with immobilized PK in the absence (A) or presence (B) of excess PLP (2 mM). The interactions were carried out at a flow rate of 8 μl/min and with an association phase of 3 min and dissociation phase of 5 min. The residual plots with minimum χ^2 values of fitting are shown in the lower panel. Non-linear regression analysis of the association and the dissociation curves was performed using the simple one-to-one binding model. Solid lines are theoretical curves based on the one-to-one binding model. The residual plot of the analysis using the heterogeneous analyte model is included for comparison.

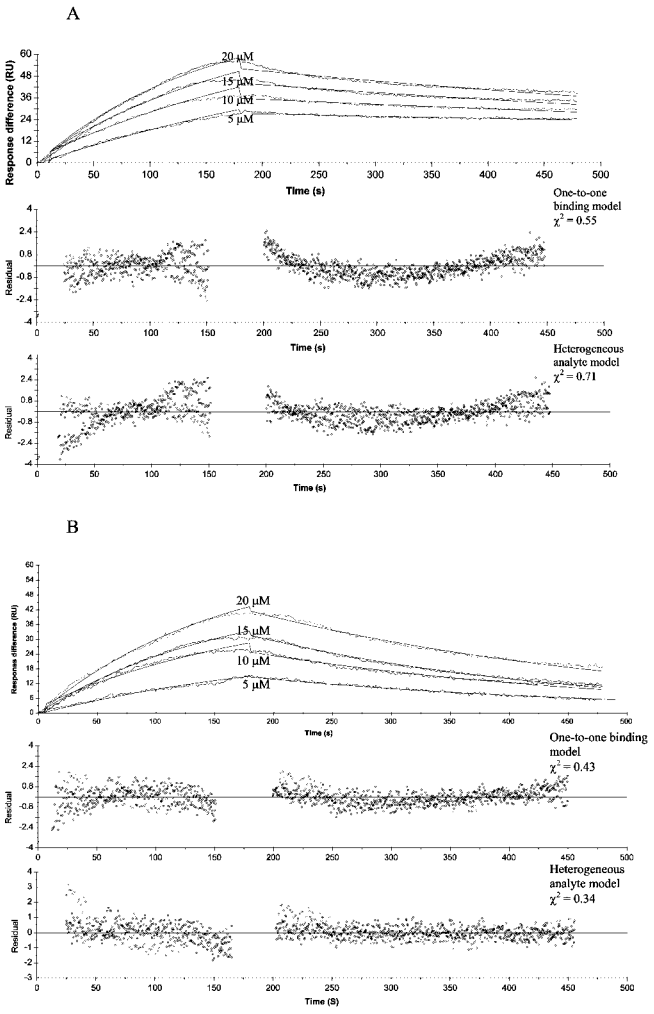

Fig. 5. **Sensorgrams showing the binding interactions of GAD with the immobilized PK.** Various concentrations of GAD (5–20 μM) were allowed to interact with immobilized PK in the absence (A) or presence (B) of excess PLP (2 mM). The interactions were carried out at a flow rate of 8 μl min and with an association phase of 3 min and the dissociation phase of 5 min. The residual plots with minimum χ^2 values of fitting are shown in the lower panel. Non-linear regression analysis of the association and the dissociation curves was performed using a simple one-to-one binding model. Solid lines are theoretical curves based on the one-to-one binding model. The residual plot of the analysis using the heterogeneous analyte model is included for comparison.

injected onto the sensor surface. Specific binding of ALT and GAD to immobilized PK is clearly shown in Fig. 3. The result suggests that binding of PLP-dependent enzymes to PK is a general event, and this finding agrees with that of the fluorescence polarization study. It appears that the higher molecular weight of GAD (as compared to ALT) contributes to the higher observable binding of GAD to immobilized PK (Fig. 3). In addition, both enzymes could bind to PK in the presence of excess PLP, which affected their binding interactions (Fig. 3).

We then determined the binding kinetics of ALT and GAD for PK by monitoring the binding interactions of different concentrations of the two enzymes to immobilized PK. Samples ranging from 5 μM to 20 μM were injected either in the presence or absence of excess PLP (2 mM). The interactions of PK-ALT and PK-GAD in the absence (A) or presence (B) of PLP are shown in Figs. 4 and 5, respectively. Both PLP-dependent enzymes bind to PK in the presence or absence of PLP. The interaction between PK with ALT and GAD increased with an increase in ALT and GAD concentrations. When PLP was added, the binding profiles of ALT and GAD with PK were affected. Excess PLP was used to ensure all the enzymes are covalently linked to their cofactor, as the majority of the enzymes are in their apo form (*31*). In the presence of

Table 1. **The association and dissociation rate constants and equilibrium affinity constants of alanine aminotransferase (ALT) and glutamate decarboxylase (GAD) for pyridoxal kinase (PK) in the presence or absence of pyridoxal-5-phosphate (PLP).**

	k_a (M^{-1} s^{-1})	k_d ($\times 10^{-4}$ s^{-1})	K_A ($\times 10^4$ M^{-1})	K_D ($\times 10^{-6}$ M)	χ^2
ALT	155	7.6	20.4	4.9	0.21
			17.9[a]	5.6[a]	
ALT + 2 mM PLP	175	26.3	6.7	15	0.33
GAD	274	7.4	37	2.7	0.55
			43.5[a]	2.3[a]	
GAD + 2 mM PLP	540	25.9	20.8	4.8	0.43

[a]Apparent equilibrium constant obtained through fluorescence polarization study.

PLP, the slopes of the association and dissociation phases for both enzymes with PK were steeper than that in the absence of PLP. Yet another study by Kawasaki (*32*) had indicated that dopa decarboxylase was 90% saturated instead of 10–20% saturated with PLP. Thus electrospray ionization time of flight mass spectrometry (ESI-Q-TOF-MS) was used to determine the mass of GAD and ALT to see whether the majority of the enzyme is in apo or holo form. As PLP is covalently bound to the enzyme, the condition used for ESI-TOF-MS would not lead to its detachment from the enzyme. If the enzyme is in holo form, it would have a mass that is 247.1 Da greater than the apo form. Figure 6 is the mass spectrum for GAD, which indicates that GAD is entirely in the apo form. The result is the same for ALT (data not shown). Though our result showed that excess PLP affects the binding profile of PK with PLP-dependent enzyme, we could not exclude the possibility that the binding of PLP to the surface of GAD or ALT might alter the conformation or charges of the surface. The latter may affect the process of binding to PK, as PLP is known to form a Schiff base non-specifically with the epsilon amino group of lysine residues of proteins.

Kinetic parameters of the binding interactions were derived from the sensorgram by non-linear curve fitting with various kinetic models using BIAevaluation Software 3.0. Base on our fluorescence polarization study, the stoichiometry of the complex between PK and PLP-dependent enzymes is 1:1. Our biosensor study also indicated that the simple one-to-one binding model is adequate to fit data for both PK-ALT and PK-GAD interactions. Use of the heterogeneous analyte and two-state models did not improve the result of curve fitting. The association rate constant calculated using simultaneous k_a/k_d models depends on the dissociation rate constant. To prevent inaccuracy that might rise due to the low dissociation rate constant, the kinetic parameters were also determined by separate k_a/k_d evaluation model using BIAevaluation software 2.2. The results are similar to that derived from the simultaneous evaluation models. Thus the simultaneous one-to-one binding model was used to evaluate the kinetic parameters. The respective residual plot and minimum χ^2 were included to indicate the goodness of fitting for each pair of interactions (Figs. 4 and 5). The respective residual plot using the heterogeneous analyte model was also included in the figures (4 and 5) for comparison of fittings between different models.

The fitted kinetic values for PK-ALT and PK-GAD interactions with and without PLP are summarized in Table 1. For both PK-ALT and PK-GAD interactions, the equilibrium affinity constants (K_A) were decreased in the presence of PLP (Table 1). The measured K_A values are of similar magnitude (10^4–10^5 M^{-1}) to those for the interaction between PK and its substrates (PL, pyridoxamine, and pyridoxine) as measured previously by our group (*10*). SPR results were consistent with the results obtained in fluorescence polarization study.

Interaction of PK with PLP-Dependent Enzymes—Our results from fluorescence polarization and SPR biosensor

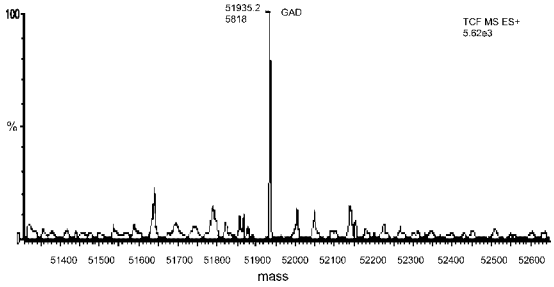

Fig. 6. **Mass spectrum for GAD using ESI-Q-TOF-MS.** GAD (10^{-4} M) was dissolved in 50% acetonitrile acidified with 1% formic acid and sprayed through capillary at a voltage range from 2.2 to 3 kV. Horse heart myoglobin was used as the standard for calibration, and the mass was scanned between 600 and 1,600 m/z.

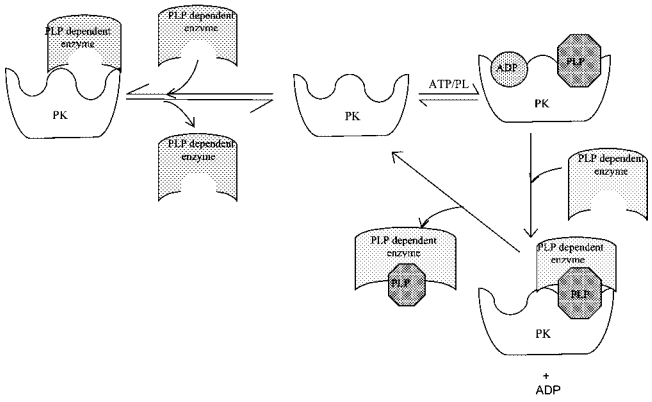

Fig. 7. **Proposed model for PLP transfer from PK to PLP-dependent enzymes.** In the presence of ATP, PL is converted to PLP and is ready for transfer. When the apo form of ALT or GAD is present, their binding to PK will allow the transfer of PLP from PK. After PLP transfer, the holo-enzyme ALT-PLP or GAD-PLP dissociates from PK, and PK is ready for another cycle of PLP transfer. In the absence of PLP, ALT or GAD can still bind to PK, but the association and dissociation rate constants are smaller than those in the presence of PLP.

studies showed that both PLP-dependent enzymes bind to PK in the presence or absence of PLP. These results support our hypothesis that PLP transfer requires the direct interactions of PK with PLP-dependent enzymes upon its biosynthesis by PK to prevent PLP depletion in the cell by phosphatase. The association constants for the interaction of PK with the two PLP-dependent enzymes are of similar magnitude, suggesting that both enzymes have similar affinity towards PK (Table 1). The affinities of the two enzymes for PK were both decreased in the presence of excess PLP, due to the dramatic increase in dissociation rate of the interactions (Table 1). The results suggest that PLP facilitates the dissociation of PLP-dependent enzymes from PK, which may in turn facilitate the access of other PLP-dependent enzymes that are in need of PLP. The slight difference between the K_D measured by the two methods might be due to the difference between the methods used i.e., fluorescence polarization study involves the attachment of a fluorescence probe to PK and is carried out in aqueous phase, while the SPR biosensor involves the immobilization of PK and is carried out on solid-liquid interface. In any case, the binding interactions will be affected to different extents.

Previous study reported that AST, another PLP-dependent enzyme, interacts specifically with PK (*13*). Together with the results obtained in the present study, the interaction of PLP-dependent proteins with PK is likely to be a process for PLP transfer. Fig. 7 is a proposed model that summarizes the major events for the coupling of PLP production by PK to its delivery to PLP-dependent enzymes. PL is converted by PK to PLP, which then interacts with PLP-dependent enzymes for direct transfer of PLP. In the presence of PLP, the dissociation of PLP-dependent enzymes from PK is enhanced, allowing the release of these enzymes from PK. In the absence of PLP, the PLP-dependent enzymes could still bind to PK, but with smaller association and dissociation rate constants. Although our data demonstrate the direct interactions between PK and PLP-dependent enzymes, it remains to be determined if the domain for PK-PLP-dependent enzymes interactions is superimposed with the catalytic domain of PK. This information will further support our hypothesis that the direct contact between PK and PLP-dependent enzymes allows PLP transfer, and provides a mechanism for how more than 100 different PLP-dependent enzymes can obtain sufficient PLP in despite the extremely low concentration of free PLP in the cell. Our model provides a possible mechanism for PLP transfer to prevent the access of existing phosphatases to the newly synthesized PLP.

This work was initiated by late Prof. J.E. Churchich and we would like to dedicate this manuscript to him in memory of his invaluable comments on this study. This project was supported by the Areas of Excellence Scheme Established under the University Grants Committee of the Hong Kong Special Administrative Region, China [AOE/P-10/01], and by the Area of Strategic Development Grant from the Hong Kong Polytechnic University A008.

REFERENCES

1. Leklem, J.E. (1991) Vitamin B_6 in *Handbook of Vitamins* (Machlin, L.J., ed.) pp. 341–392, Marcel Dekker, New York
2. Snell, E.E. (1990) Vitamin B_6 and decarboxylation of histidin. *Ann. N. Y. Acad. Sci. USA* **585**, 1
3. Denesyuk, A.I., Denessiouk, K.A., Korpela, T., and Johnson, M.S. (2002) Functional attributes of the phosphate group binding cup of pyridoxal phosphate-dependent enzymes. *J. Mol. Biol.* **316**, 155–172
4. McCormick, D.B. and Chen, H.J. (1999) Update on interconversions of vitamin B-6 with its coenzyme. *J. Nutr.* **129**, 325–327
5. McCormick, D.B., Gregory, M.E., and Snell, E.E. (1961) Pyridoxal phosphokinases I. assay, distribution, purification and properties. *J. Biol. Chem.* **236**, 2076–2082
6. Leung, Y.C., Wong, H.Y., Churchich, J.E., Lo, S.C.L., and Kwok, F. (2000) Structure-function relationships of porcine pyridoxal kinase in *Biochemistry and Molecular Biology of Vitamin B6 and PQQ-Dependent Proteins* (Iriarte, A., Kagan, H.M., and Martinez-Carrion, M., eds.) pp. 277–280, Birkhäuser Verlag, Boston
7. Li, M.H., Kwok, F.W., Chang, R., Lau, C.K., Zhang, J.P., Lo, S.C.L., Jiang, T.D., and Liang, C. (2002) Crystal structure of brain pyridoxal kinase, a novel member of the ribokinase superfamily. *J. Biol. Chem.* **277**, 46385–46390
8. Merrill, A.H. Jr., Henderson, J.M., Wang, E., McDonald, B.W., and Millikan, W.J. (1984) Metabolism of vitamin B-6 by human liver. *J. Nutr.* **114**, 1664–1674
9. Laine-Cessac, P. and Allain, P. (1996) Kinetic studies of the effects of K+, Na+ and Li^+ on the catalytic activity of human erythrocyte pyridoxal kinase. *Enzyme Protein* **49**, 291–304
10. Fong, C.C., Lai, W.P., Leung, Y.C., Lo, S.C.L., Wong, M.S., and Yang, M. (2002) Study of substrate-enzyme interaction between immobilized pyridoxamine and recombinant porcine pyridoxal kinase using surface plasmon resonance biosensor. *Biochim. Biophys. Acta* **1596**, 95–107
11. Pogell, B.M. (1958) Enzymatic oxidation of pyridoxamine phosphate to pyridoxal phosphate in rabbit liver. *J. Biol. Chem.* **232**, 761–776
12. Snell, E.E. and Haskell, B.E. (1971) The metabolism of vitamin B_6 in *Comprehensive Biochemistry* (Florkin, M. and Stotz, E.H., eds.) Vol. **21**, pp. 47–67, Elsevier, New York
13. Kim, Y.T., Kwok, F., and Churchich, J.E. (1988) Interactions of pyridoxal kinase and aspartate aminotransferase emission anisotropy and compartmentation studies. *J. Biol. Chem.* **263**, 13712–13717
14. Strausbauch, P.H. and Fischer, E.H. (1970) Chemical and physical properties of Escherichia coli glutamate decarboxylase. *Biochemistry* **9**, 226–233
15. Strausbauch, P.H. and Fischer, E.H. (1970) Structure of the binding site of pyridoxal 5′-phosphate to *Escherichia coli* glutamate decarboxylase. *Biochemistry* **9**, 233–238
16. Wu, J.Y., Denner L., Lin, C.T., and Song, G. (1985) L-Glutamate decarboxylase from brain. *Methods Enzymol.* **113**, 3–10
17. DeRosa, G. and Swick, R.W. (1975) Metabolic implications of the distribution of the alanine aminotransferase isoenzymes. *J. Biol. Chem.* **250**, 7961–7967
18. Chaiken, I., Rose, S., and Karlsson, R. (1992) Analysis of macromolecular interactions using immobilized ligands. *Analy. Biochem.* **201**, 197–210
19. Fägerstam, L. (1991) A non-label technology for real-time biospecific interaction analysis in *Techniques in Protein Chemistry II* (Villafranca, J.J. ed.) pp. 65–71, Academic Press, New York
20. BIAtechnology Handbook, Biacore AB, Uppsala, Sweden
21. Myszka, D.G. (1997) Kinetic analysis of macromolecular interactions using surface plasmon resonance biosensors. *Curr. Opin. Biotechnol.* **8**, 50–57
22. Schuck, P. (1996) Kinetics of ligand binding to receptor immobilized in a polymer matrix, as detected with an evanescent wave biosensor. I. A computer simulation of the influence of mass transport. *Biophys. J.* **70**, 1230–1249

23. BIAcore X Instrument Handbook, Phamacia Biosensor AB Press, Uppasla, Sweden
24. Wong, M.S., Fong, C.C., and Yang, M. (1999) Biosensor measurement of the interaction kinetics between insulin-like growth factors and their binding proteins. *Biochim. Biophys. Acta* **1432**, 293–301
25. Huang, M., Lai, W.P., Wong, M.S., and Yang, M. (2001) Effect of receptor phosphorylation on the binding between IRS-1 and IGF-1R as revealed by surface plasmon resonance biosensor. *FEBS Lett.* **505**, 31–36
26. BIAevaluation version 3.0 software handbook, Phamacia Biosensor AB Press, Uppsala, Sweden.
27. Karlsson, R. (1994) Real-time competitive kinetic analysis of interactions between low-molecular-weight ligands in solution and surface-immobilized receptors. *Anal. Biochem.* **221**, 142–151
28. BIAevaluation version 2.2 software handbook, Phamacia Biosensor AB Press, Uppsala, Sweden.
29. Li, T.K., Lumeng, L., and Veitch, R.L. (1974) Regulation of pyridoxal 5′-phosphate metabolism in liver. *Biochem. Biophys. Res. Commum.* **61**, 677–684
30. Stenberg, E., Persson, B., Roos, H., and Urbaniczky, C. (1991) Quantitative determination of surface concentrations of protein with surface plasmon resonance using radiolabeled proteins. *J. Coll. Interface Sci.* **143**, 513–526.
31. Qu, K., Martine, D.L., and Lawrence, C.E. (1998) Motifs and structural fold of the cofactor binding site of human glutamate decarboxylase. *Protein Sci.* **7**, 1092–1105
32. Kawasaki, Y., Hayashi, H., Hatakeyama, K., and Kagamiyama, H. (1992) Evaluation of the holoenzyme content of aromatic L-amino acid decarboxylase in brain and liver tissues. *Biochem. Biophys. Res. Commun.* **186**, 1242–1248